J. Geomag. Geoelectr., **40**, 1481–1501, 1988

Geophysical Study of Two Seamounts near Minami-Tori Sima (Marcus) Island, Western Pacific Ocean

Yoshio UEDA

Hydrographic Department, 5-3-1, Tsukiji, Chuo-ku, Tokyo 104, Japan

(Received April 13, 1988; Revised August 30, 1988)

Sea-bottom topography, magnetic and gravity anomaly maps were compiled for two seamounts, Smt-948 (23.7°N, 151.9°E) and Smt-1100 (22.8°N, 153.4°E) in the vicinity of Minami-Tori Sima (Marcus) Island based on survey data observed by the S/V Takuyo of the Hydrographic Department of Japan from July to August, 1985. These flat-topped seamounts are located in the Jurassic magnetic quiet zone on crust older than 150 Ma. On Smt-1100, sea bottom photographs were taken with a deep-sea camera and three dredge hauls were made. Three-dimensional magnetic analyses of Smt-948 gave a paleomagnetic pole position of 57.5°N, 329.5°E with the goodness-of-fit ratio 2.83. The pole position lies in the Pacific apparent polar wander path between the Late Jurassic (150 Ma) and the Late Cretaceous (65–94 Ma). This result implies that Smt-948 was generated in the middle Cretaceous, a significant period after the formation of the Jurassic sea-floor. Two-dimensional modeling of magnetic and gravity anomalies across these seamounts reveal a caldera-like basement structure, suggesting a constructional origin of the flat top of the guyot. A sequence of normal and reversed magnetic polarity layers is estimated from magnetic modeling on Smt-1100.

1. Introduction

The Hydrographic Department of the Maritime Safety Agency, Japan (hereinafter referred to as JHD) conducted bathymetric, magnetic and gravity surveys on two seamounts near Minami-Tori Sima Island (Marcus Island) by the S/V Takuyo from July to August 1985. One of these seamounts, named Smt-948 after its summit depth, is located at 23°40′N, 151°55′E about 120 miles west to southwest of Minami-Tori Sima Island. The other seamount, named Smt-1100, is located at 22°50′N, 153°25′E, about 90 miles southwest of Minami-Tori Sima Island. SMOOT (1983) has published detailed multibeam sonar maps of this seamount giving its name as "Jaybee". Both seamounts are guyots and repose on sea floor from the Jurassic magnetic quiet zone. At the summit of Smt-1100, sea-bottom photographs were made at two sites with a deep-sea camera and three dredge hauls were obtained at these two and an additional site. The results of the surveys are thought to be significant for consideration of tectonics and the origin of guyots and magnetic quiet zones in the Jurassic age. This paper describes the survey results and

presents magnetic and gravity models of the guyots with a discussion of paleomagnetic implications derived from magnetic analysis.

2. Survey

A generalized topographic map of the seamounts discussed here is shown in Fig. 1 along with geophysical tracklines. Navigation was controlled by an integrated navigation system using doppler satellite positioning, inertial navigation, and Loran C. A sea-beam system operating at 12.158 kHz was used during the cruise and a preliminary bathymetric chart of the surveyed area was drawn onboard. Soundings

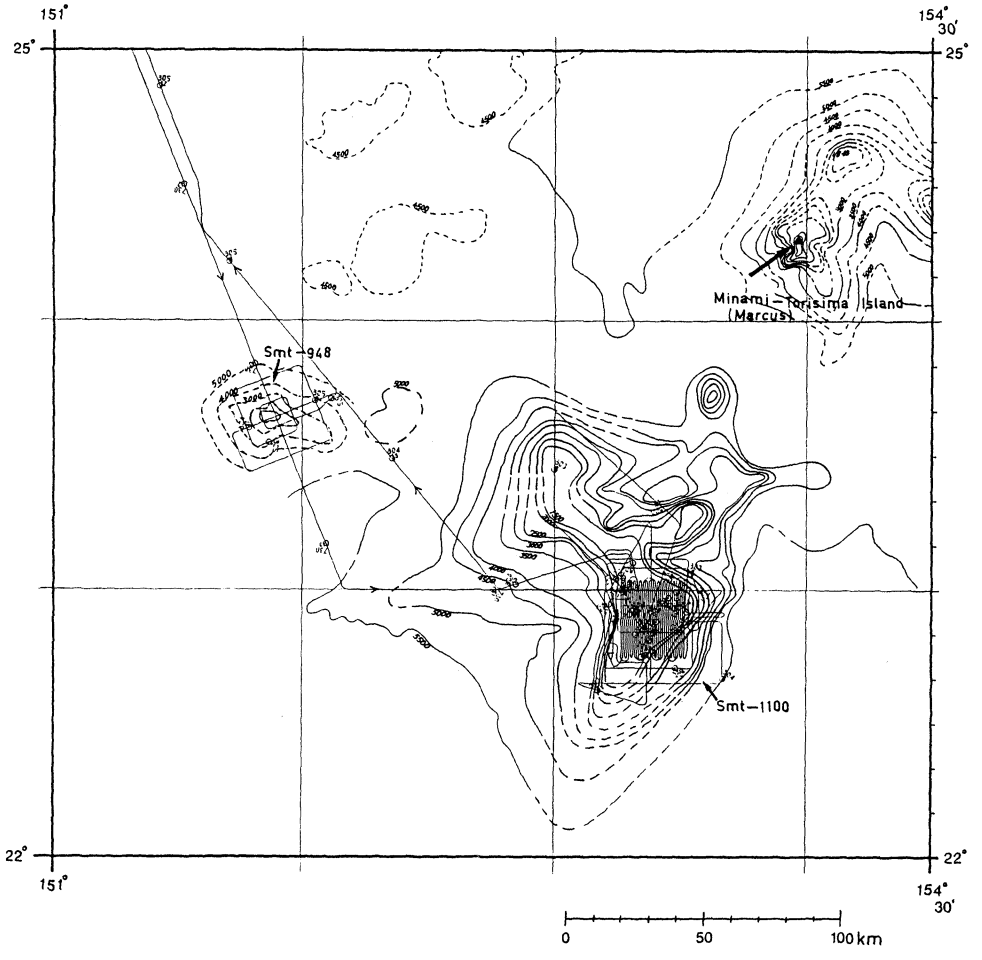

Fig. 1. Bathymetric map of two seamounts near Minami-Tori Sima (Marcus) Island, from the bathymetric chart "G1604, G1605" compiled by JHD. Light solid lines indicate ship track lines. Contour interval is 500 m.

were corrected for sound velocity in seawater by Wilson's formula (WILSON, 1960). Total magnetic intensity was measured with a proton precession magnetometer, towed about 300 m behind the ship. External field corrections were made using hourly mean data recorded at the Chichijima magnetic observatory (27.1°N, 142.2°E) operated by the Meteorological Agency of Japan. The external magnetic variation was generally small, as noted from the K index, which was less than 3 during the magnetic surveys on the seamounts. A total intensity magnetic anomaly was calculated by subtracting the IGRF 1980 model from the observed magnetic values. Gravity was measured using a KSS-30 marine gravity meter manufactured by the Bodenserwerk Co. of West Germany. Mean drift of the gravity meter was less than 1.5 mgal/month. Observed gravity values were converted to the absolute gravity values based on the Japan Gravity Standardization Net 1975 (GEOGRAPHICAL SURVEY INSTITUTE, 1976). Free-air gravity anomaly values were calculated by subtracting normal gravity values based on the international geodetic reference system, 1967.

3. Geophysical Study of Smt-948

3.1 Bathymetry

A bathymetric contour map of Smt-948 is shown in Fig. 2(a). Smt-948 rises from average surrounding depths of 5500 m to a minimum depth of 948 m, giving a total height of 4552 m. The top of the seamount is nearly flat. The shape of Smt-948 is oval with a major axis of 63 km running ESE, and a maximum width of 42 km. A slope break occurs at around the 1500 m depth on the flanks and the maximum slope angle reaches 30 degrees. A radial fissure pattern appears to be developed around the summit area.

3.2 Geomagnetic study

3.2.1 Magnetic anomaly

The magnetic anomaly of Smt-948 (Fig. 2(b)) is elongated in the ESE direction in agreement with the topography. A negative anomaly zone is predominant over the uplift of the seamount indicating a generally normal polarity. The largest negative anomaly peak of −820 nT is found over the upper southern slope and another peak of −700 nT is recognized over the upper northern slope. In between is a relatively high anomaly amounting to 400 nT.

3.2.2 3D-magnetic analysis

The mean magnetization vector of a seamount can be calculated by Talwani's method, on the assumption of a uniform magnetization of the source body (TALWANI, 1965). In this method, a seamount is approximated by a stack of polygons following the contour lines of the bathymetric map and a magnetization vector, $\boldsymbol{J}$, and a planar trend are calculated by minimizing the square summation of residuals between observed and calculated anomalies. To examine the fit of the observed and calculated anomalies, the goodness of fit ratio G, mean absolute residual (Res) and root mean square (rms) residual were calculated (UYEDA and

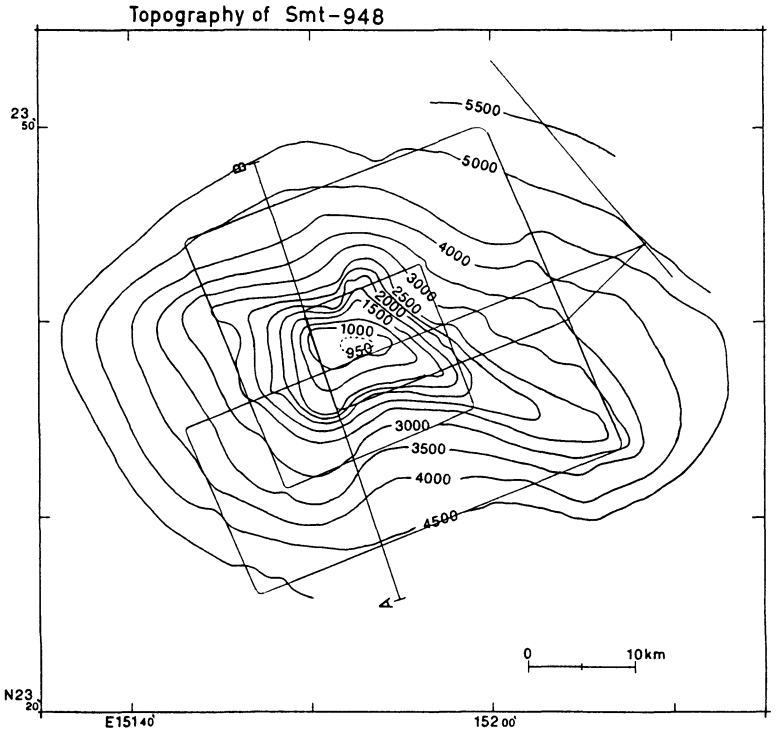

(a)

Fig. 2. Topography and magnetic/gravity anomaly of Smt-948. Profile along line A–B was subject of two-dimensional magnetic/gravity analysis. (a) Topography of Smt-948. Contour interval is 500 m. Track lines are superimposed on contour map as light solid lines. (b) Total intensity magnetic anomaly of Smt-948. Contour interval is 100 nT. (c) Free-air gravity anomaly of Smt-948. Contour interval is 10 mgal.

RICHARDS, 1966; RICHARDS *et al.*, 1967; HARRISON, 1971). In general, magnetic analyses whose *G*-ratios are less than 1.8 are not accepted as reliable results suitable for paleomagnetic study (HARRISON *et al.*, 1975).

Calculations were performed with several models of the seamount and the results are listed in Table 1. Taking into account the thickness of the sediment layer, the base of the model was extended from 5500 m to 6250 m (model 2 in Table 1). Additionally, the top portion of the seamount was truncated gradually to improve the *G*-ratio, as has been commonly done with other Pacific seamounts (HARRISON, 1971; HARRISON *et al.*, 1975). The maximum *G*-ratio for Smt-948 (2.83) was obtained when the uppermost 2500 m was removed (model 3 in Table 1). Figures 3(a) and 3(b) show the computed anomaly and the residual for this model; however, even the nonmagnetic summit of model 3 could not accurately simulate the bimodal negative peak. Model 4 in Table 1 shows the result when the magnetization of the

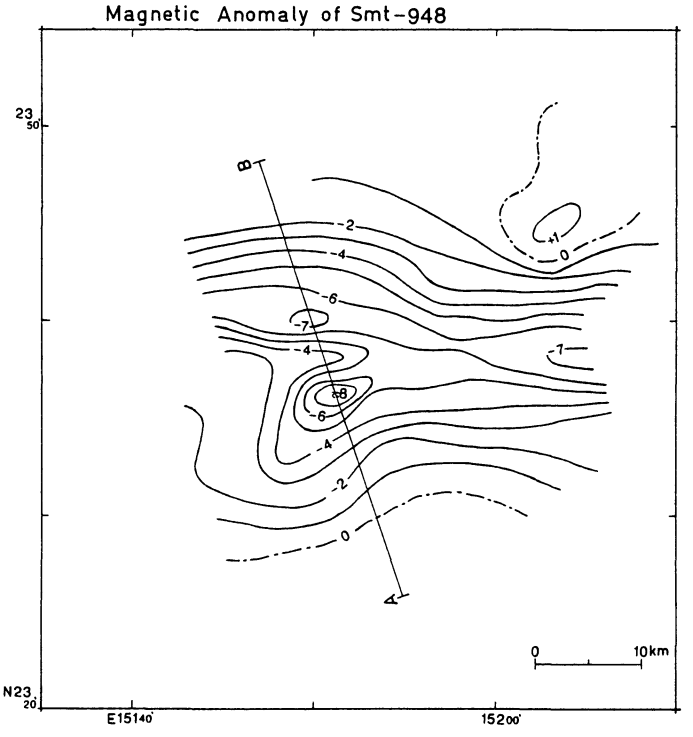

(b)

Fig. 2. (continued).

top and bottom portions were solved for independently. This model also failed to produce a bimodal negative anomaly shape. Judging from the above results, it appears that the magnetic structure of Smt-948 is more complex than can be reproduced with simple 3D models. A more detailed study of the structure of this seamount, derived from two-dimensional analysis, is described in the following section.

Although the fit of the observed and calculated anomalies is not perfect, the *G*-ratio of model 3 satisfies Harrison's acceptance criteria permitting the use of the result for paleomagnetic considerations. The magnetization direction of model 3 (Table 1) was Inc=−17.5°, Dec=1.3° with a magnetization intensity of 5.1 A/m. The paleolatitude derived from the magnetization is 9.0°S and the paleomagnetic pole is located at 57.3°N, 329.5°E. This paleolatitude implies that Smt-948 was created in the southern hemisphere and then drifted northward by as much as 30

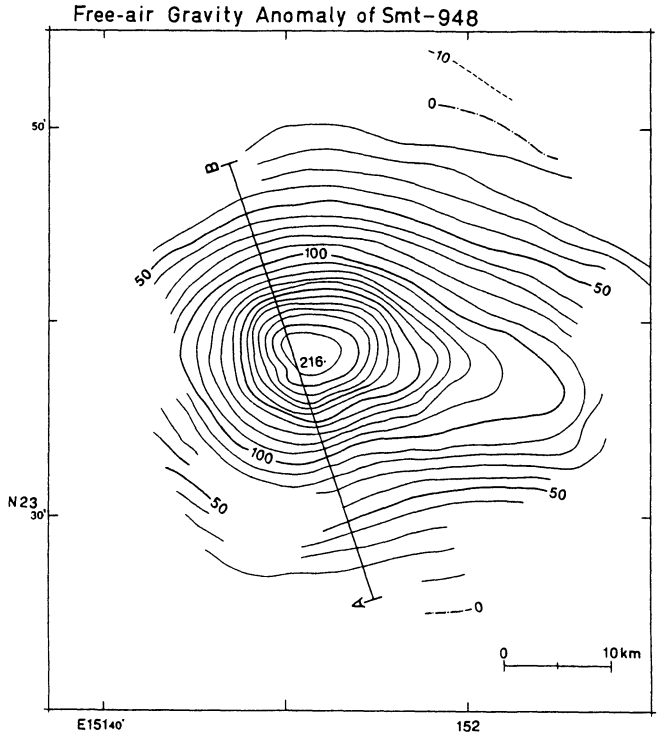

(c)

Fig. 2. (continued).

degrees in accordance with published observations of Pacific plate motion (HARRISON *et al.*, 1975). On the other hand, the paleopole position of Smt-948 agrees well with the average pole (52.7°N, 340.9°E) of the Wake seamount group as well as the pole of Makarov guyot (63.7°N, 331.3°E) which belongs to the South Japanese Group. OZIMA *et al.* (1977) reported the radiometric age of the guyots in the Western Pacific. According to their results, the ^{40}Ar–^{39}Ar age of Makarov Guyot is 94 Ma, and other guyots belonging to the Wake guyots near Smt-948 also fall in the range between 86 Ma and 98 Ma. From these results, it appears to be plausible that Smt-948 was generated during the Middle Cretaceous and recorded the paleomagnetic pole in accordance with the South Japanese Group. Further discussion of the paleomagnetic pole of Smt-948 is described in Section 5.

3.2.3 Magnetic structure

As was mentioned in the previous section, Smt-948 has a bimodal negative anomaly pattern over the uplift. To investigate the magnetic structure producing this anomaly, a two-dimensional analysis on profile A–B in Fig. 2(b) was conducted. The model structure was revised by a trial and error method until the agreement

Table 1. Results of three-dimensional magnetic analyses of Smt-948 (23.7°N, 151.9°E).

Model description			Magnetization vector							trend			Paleo-Lat.	Paleopole	
Model No.	Top (m)	Base (m)	Dec (°)	Inc (°)	SDa (°)	Intensity A/m	SDm A/m	G-ratio	/Res/ nT	North (nT/km)	East (nT/km)	Bias nT	Lat. (°)	Lat. (°)	Lon. (°)
1 topographic	950	5500	13.8	−11.4	3.4	3.4	0.2	2.01	91.6	2.3	0.3	−208	−5.8	57.6	305.6
2 Bottom extended	950	6250	14.5	−12.8	3.3	3.4	0.1	2.09	92.7	2.3	0.3	−139	−6.5	56.7	305.0
3 Top trancated	2500	6250	1.3	−17.5	3.0	5.1	0.3	2.83	77.0	1.0	−1.0	−9.2	−9.0	57.3	329.5
4 Two layers	950	2500	73.6	−10.7	18.0	9.4	0.3	2.83	76.4	1.1	−1.0	−16.5	****	****	****
	2500	6250	−1.1	−16.9	3.3	5.0	0.3						−8.6	57.6	333.9

*Standard deviation of magnetization vector (FRANCHETEAU *et al.*, 1970).

Mean paleopole position of above results, calculated by Fisher's average method, is 58.0°N, 320.6°E, with 95 percent confidence circle of 4.5°. Goodness-of-fit ratio was used as weight factor in this calculation.

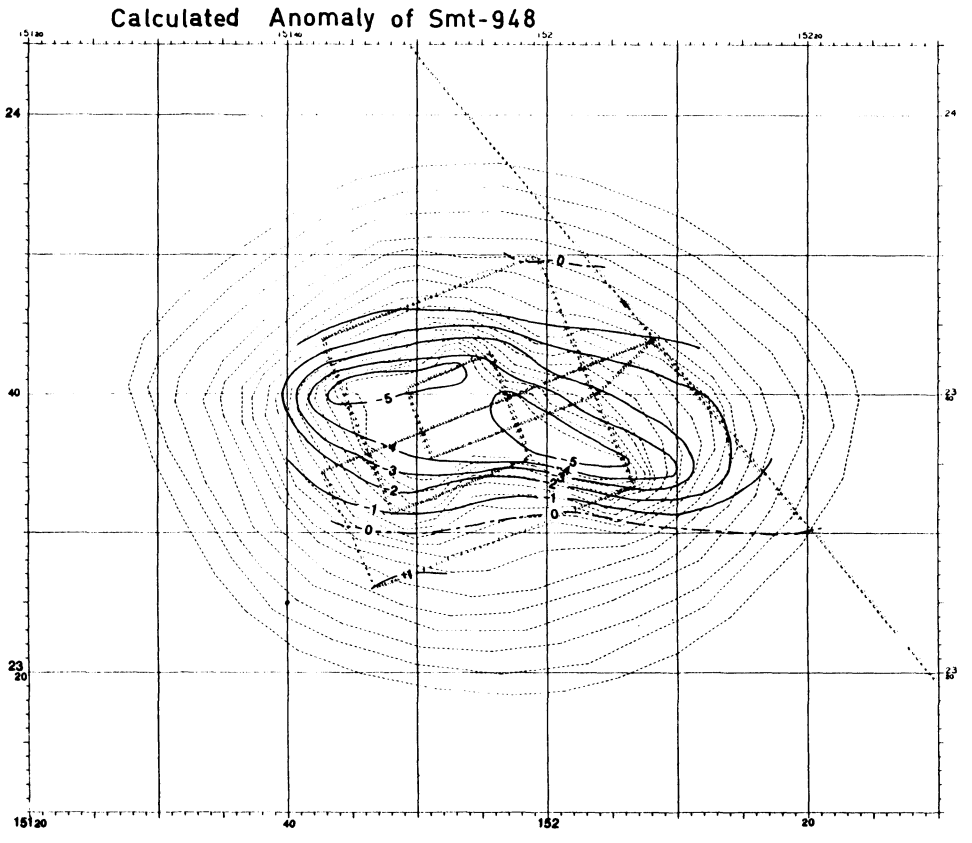

(a)

Fig. 3. Three-dimensional magnetic analysis of Smt-948. Contour interval is 100 nT. Magnetic contour lines are shown by thick lines, and three-dimensional model used for analysis is shown by dot lines. (a) Calculated anomaly of model 3 (Table 1). (b) Residual field of model 3 (Table 1), dark areas are positive residuals.

between observed and calculated anomalies became acceptable. Results of these calculations and a model obtained with this procedure are shown in Fig. 4(a). This model suggests that the normally polarized magnetic basement of Smt-948, with an intensity of 3.3 A/m, is depressed as much as 1.8 km beneath the flat top and capped by a nearly nonmagnetic layer infilling the depression structure. A similar magnetic basement structure was also reported for seamount Daiiti-Kasima (UEDA, 1985). HARRISON (1971) discovered the nonmagnetic top structure of seamounts from magnetic analysis of the seamount in the Gulf of Guinea, and ascribed this structure to the hyaloclastite resulting from alteration of basaltic lava covering the summit of the seamount. In Harrison's hypothesis, we may expect a relatively low gravity density layer at the summit of the seamount, which corresponds to the nonmagnetic

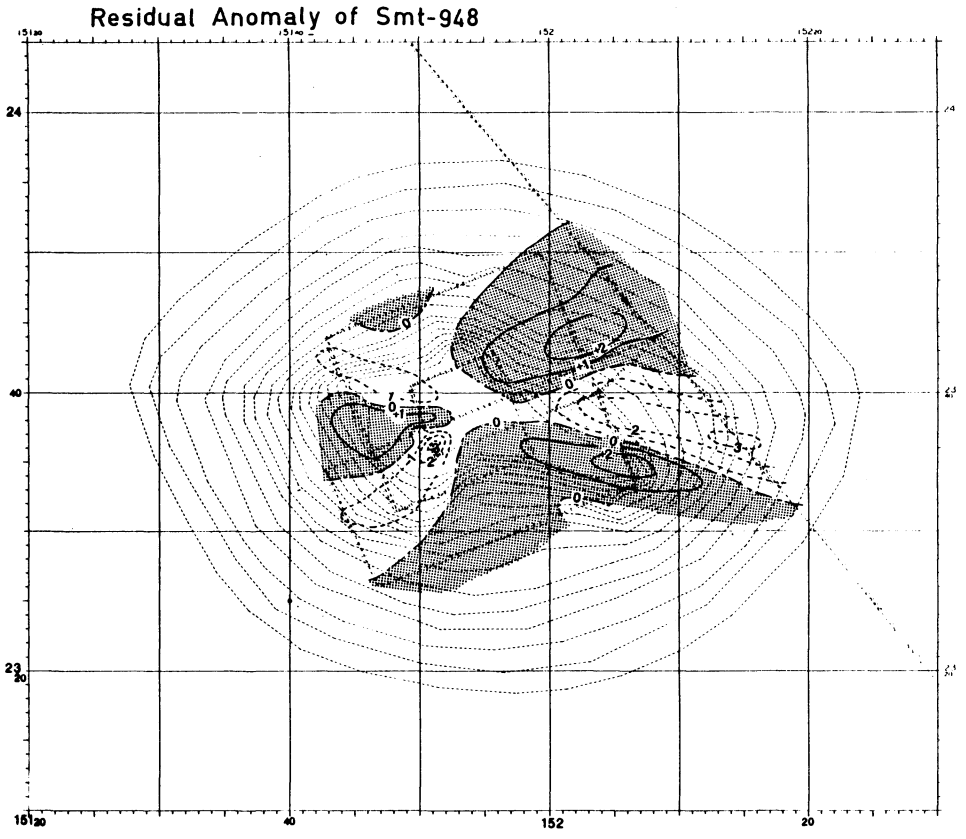

(b)

Fig. 3. (continued).

part. However, the gravity anomaly (Fig. 2(c)) shows no depression over Smt-948, which suggests that this seamount has a uniform density structure. These observations support the idea that the top portion of Smt-948 is constructed of nonmagnetic lavas. Such a magnetic structure implies an alternative origin for flat top seamounts other than the usual hypothesis of shallow water erosion (NAYUDU, 1962).

3.2.4 Gravity study

A free-air gravity anomaly map of Smt-948 is shown in Fig. 2(c). In general, the free-air anomaly is consistent with the bathymetry. A maximum of 216 mgal is found over the summit and the ESE extension of the gravity high is located slightly to the north of the topographic high, consistent with the magnetic anomaly. It is noted that the positive anomaly is flanked by a negative anomaly amounting to −10

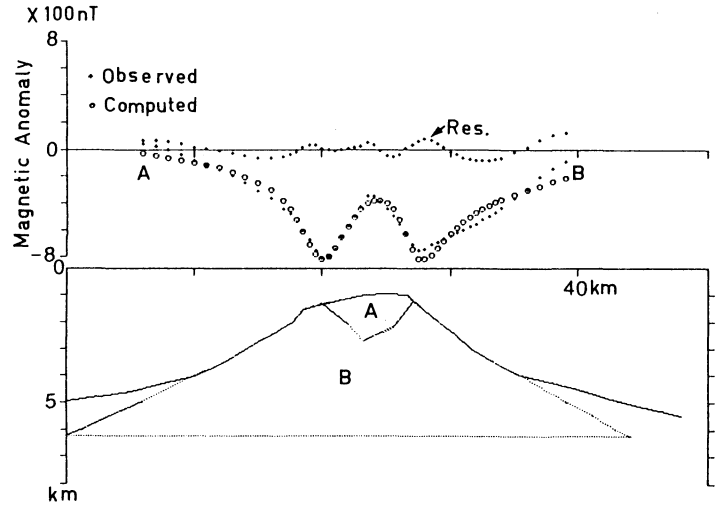

(a)

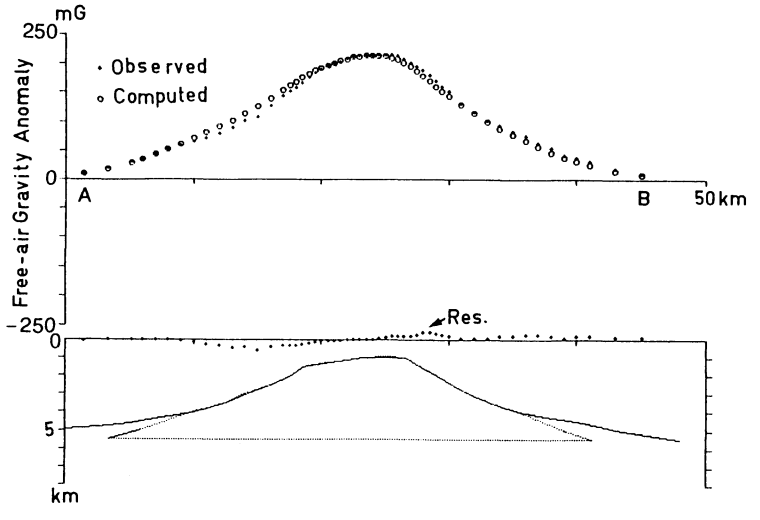

(b)

Fig. 4. Results of two-dimensional magnetic/gravity analyses of Smt-948. (a) Two-dimensional magnetic analysis of a profile along line A–B of Fig. 2(b). Solid cross marks mean observed anomalies and open circles are calculated anomalies. Residuals are also shown by solid cross marks. Magnetization intensity and effective inclination of A is 0.28 A/m, −113° and those of B 3.28 A/m, −12°. Goodness-of-fit ratio is 7.6. (b) Two-dimensional gravity analysis of a profile along line A–B of Fig. 2(c). Solid cross marks mean observed anomalies and open circles are calculated anomalies. Residuals are also shown by solid cross marks. Calculated mean density is 2.55 g/cc. Goodness-of-fit ratio is 22.4.

mgal. The gravity anomaly profile A–B in Fig. 2(c) is analyzed with a two-dimensional method to estimate the mean density of the seamount. The result of the analysis is illustrated in Fig. 4(b). The calculated densities varied from 2.55 g/cc to 2.43 g/cc, when the basement depth was extended from 5500 m to 6250 m. Using a 2-D analysis for a 3-D seamount will tend to slightly overestimate the volume of the seamount and hence underestimate the density; however, the calculated values are in good agreement with those of other Pacific seamounts (LEPICHON and TALWANI, 1964; SCHIMKE and BUFE, 1968; SAGER *et al.*, 1982). The gravity model shows no caldera depression, which might suggest that magnetic features over the summit do not reflect density contrast, but rather the same density material with a different magnetization.

4. Geophysical Study of Smt-1100

4.1 Bathymetry

Sea-beam topography of Smt-1100 is shown in Fig. 5(a). Smt-1100 is a southern extension of a larger seamount, which may consist of three small seamounts as shown in Fig. 1 (SMOOT, 1983). Several flat plains are observed in the summit area at a depth between 1100 m and 1400 m. The flat plain at the depth around 1100 m is 11 km wide in the E-W direction and 13 km wide in the N-S direction. Four small volcanic knolls with heights of about 100 m are located on the flat plain. A slope break occurs on the flanks at a depth between 1360 m and 1380 m and the maximum slope reaches more than 30 degrees. Sea-bottom photographs were taken at sites A and C, and dredge hauls were made at sites A, B and C (Fig. 5(a)). Figure 6 shows photographs from sites A and C. Dull yellow silty sand containing small debris and a number of nanno-fossils were dredged from site A (22°50.9′N, 53°21.4′E, depth=1138 m). The photograph from site A (Fig. 6(a)) indicates that basement rock protrudes to the sea-bottom surface in places among the sand layers. Manganese-coated debris were dredged from site B (22°56.0′N, 153°22.7′E, depth=955 m) on the summit of a small knoll. The cores of the manganese nodules were mainly composed of tuff breccia. Site C (22°58.1′N, 153°17.3′E, depth=1570 m) was located on the upper western slope at the 1570 m depth. A large manganese crust, greater than 20 cm in diameter, was dredged along with small sub-rounded basaltic conglomerates. The sea-bottom photograph from site C (Fig. 6(b)) also shows a wide distribution of manganese crusts. It is noteworthy that no coral materials were found on the summit of Smt-1100.

4.2 Magnetic/gravity anomaly

The total magnetic intensity anomaly map of Smt-1100 is illustrated in Fig. 5(b). A negative anomaly is predominant over the uplift and positive zones are restricted to a small area. The magnetic anomaly of this seamount is probably too complicated to be approximated by a uniform magnetization model (MCNUTT, 1986). Several negative anomaly zones trending ENE-WSW are recognized and a positive zone is located over the central part of the flat top surface, where a relative

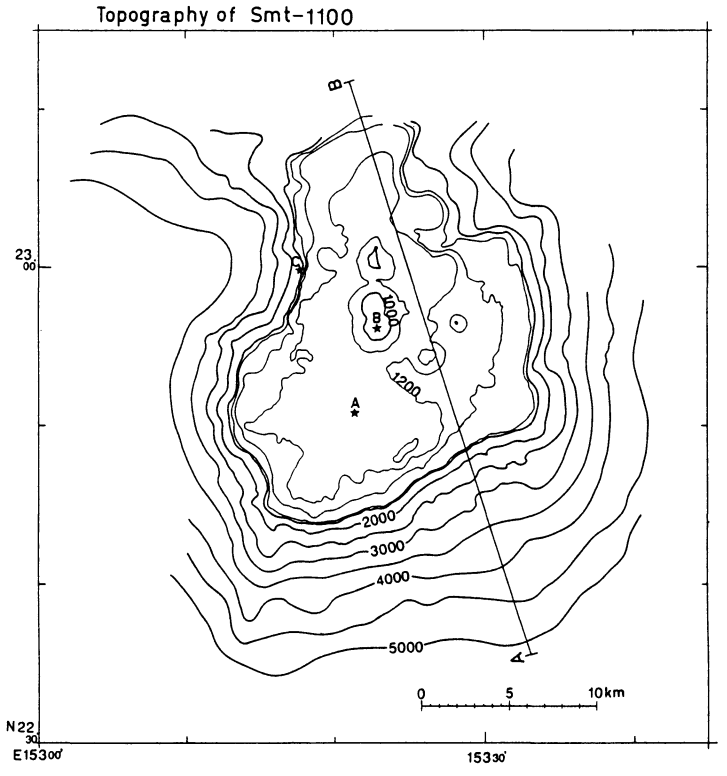

(a)

Fig. 5. Topography and magnetic/gravity anomaly of Smt-1100. Profile along line A–B was subject of two-dimensional magnetic/gravity analysis. (a) Topography of Smt-1100. Contour interval is 500 m. Topography shallower than 1500 m is shown by contour lines with 100 m intervals. Three dredge hauls were made at sites A, B and C and photographs were made at sites A and C. (b) Total intensity magnetic anomaly of Smt-1100. Contour interval is 100 nT. Positive anomaly zones are shown by stippled pattern. (c) Free-air gravity anomaly of Smt-1100. Contour interval is 10 mgal.

gravity high is distributed corresponding to a positive magnetic anomaly zone (Fig. 5(c)). The amplitude of the magnetic anomaly ranges from 500 nT to 1100 nT. The gravity anomaly is oval in plain and has a long axis in the N-S direction following the topography. The maximum gravity anomaly of 267 mgal is found over the central part of the flat top surface and another peak of 222 mgal is recognized on the northern part of this seamount. A small basin structure is suspected between the two gravity peaks.

4.3 Two-dimensional modeling

Using the gravity and magnetic profiles along line A–B in Figs. 5(b) and 5(c), two-dimensional analyses were conducted to obtain some constraints on the internal

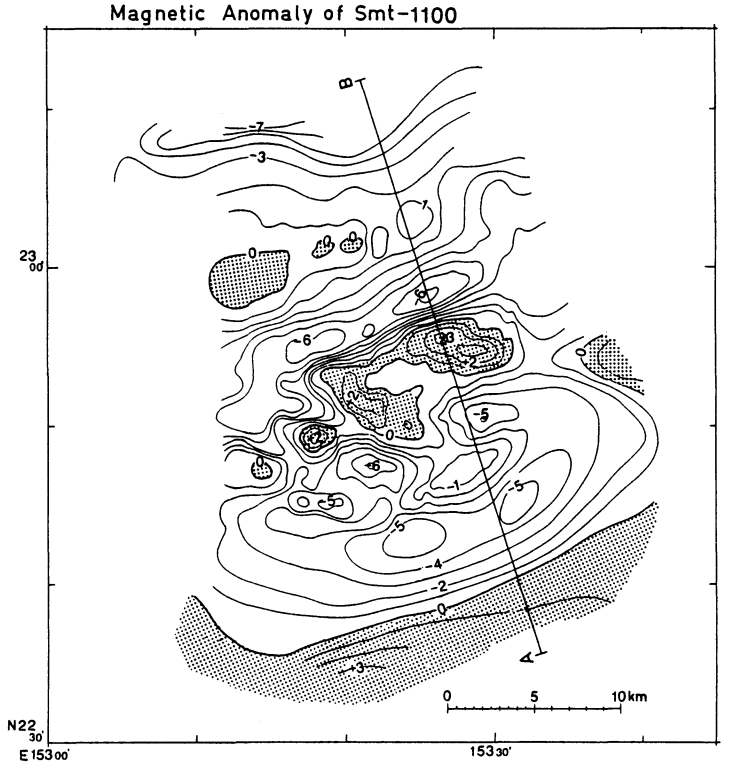

(b)

Fig. 5. (continued).

structure of Smt-1100. Model A in Fig. 7(a) shows results of the two-dimensional modeling of gravity by using the assumption of a uniform density contrast. The mean densities ranged from 2.78 g/cc to 2.82 g/cc, when the base depth was extended from 5500 m to 6250 m. Although the agreement of the observed and calculated anomalies was acceptable, positive and negative residuals amounting to several tens of mgal occurred over the flat top surface, presumably reflecting basement undulation. To improve the model, high and low density zones were assigned in model B, which may have their own density contrasts in the least squares inversion. The density of the basement of Smt-1100 became 2.82 g/cc. That of the high density part was 3.33 g/cc and the low density part was 1.55 g/cc. Though the value of the densities in model B vary depending on the arbitrary selection of the

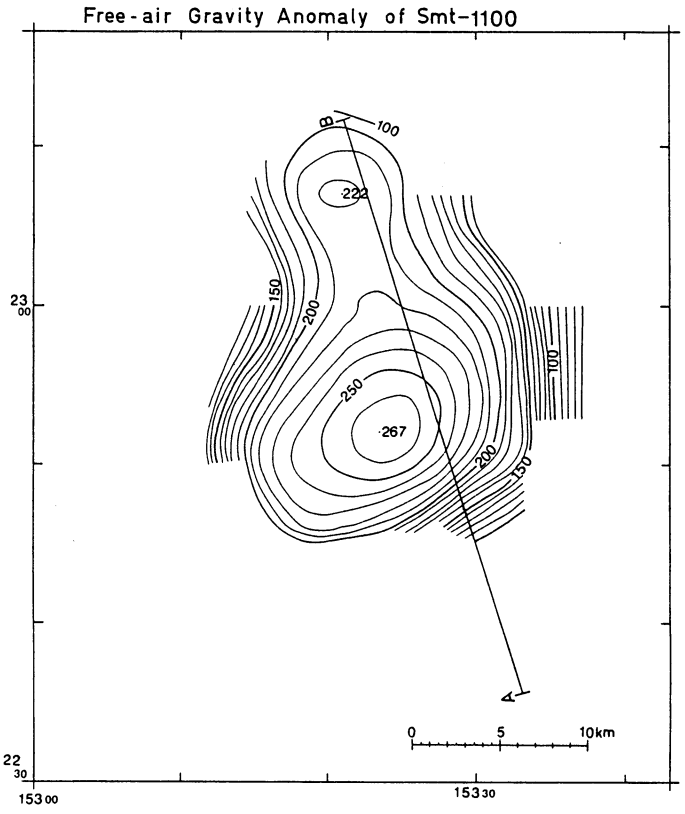

(c)

Fig. 5. (continued).

shape and thickness of the high and low density bodies, it seems significant that the high density zone is located below the southern part of the flat top surface in agreement with the relative magnetic high. The density of the basement of Smt-1100 is also considerably larger than the density value of Smt-948 (2.55 g/cc) and other seamounts, reflecting a source material rich in basic composition. Another characteristic feature of model B is an undulated relief of the boundary between the basement and the high/low density zones. This feature suggests volcanic activity filling a depressed zone, which resulted in flat top formation.

Magnetic analysis was carried out based on the same model derived from gravity analysis, with some modifications, as shown in Fig. 7(c). In the model calculation, we used the result of two-dimensional magnetic analysis of nearby seamount Smt-948 and assumed that the effective inclination of magnetization for Smt-1100 was $-12°$. Figure 7(c) shows that the high and low density zones are reversely magnetized with intensities of 2.42 A/m and 1.30 A/m respectively. The

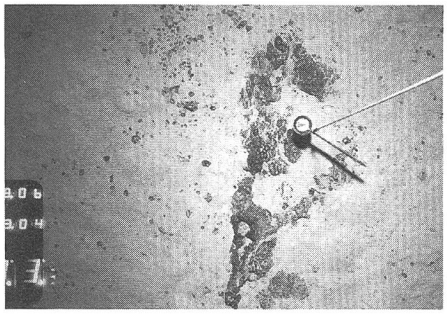

(a)

(b)

Fig. 6. Sea bottom photographs of Smt-1100. (a) Photograph from site A (Fig. 5(a)), located on the flat top at 1138 m depth. (b) Photograph from site C (Fig. 5(a)), located on the upper western slope at 1570 m depth.

basement of Smt-1100 has a magnetization intensity of 1.83 A/m in a normal direction. Beneath the southern slope of the uplift, a normally magnetized body with 5.40 A/m intensity is estimated. In general, the magnetization intensities derived from the above analysis were small, except for the body beneath the southern slope. The magnetization intensities of dredged basaltic rocks from site C (Fig. 5(a)) ranged from 5.5 A/m to 8.2 A/m (Utasiro, S., personal communication). This value is considerably larger than that of the model analysis. Such a large magnetization intensity may occur by ascribing the anomaly only to a normal magnetization of the basement; however, an extraordinary undulation of the magnetized body is needed in this case. Although it is difficult to solve this paradox, we assume that the dredged samples do not represent the total picture but were from a restricted section with a strong magnetization. It is widely expected that seamounts formed in the magnetic quiet zone were magnetized in a normal epoch; however, this analysis of Smt-1100 indicates the existence of a reversely magnetized section with weak intensity.

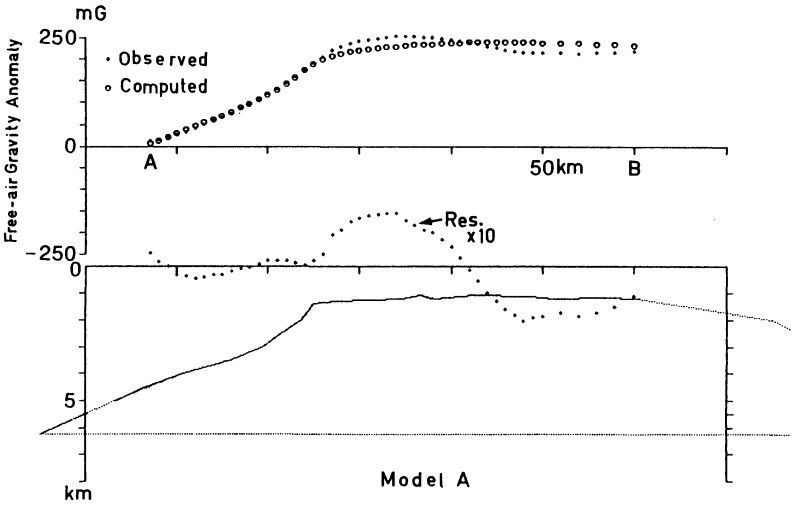

(a)

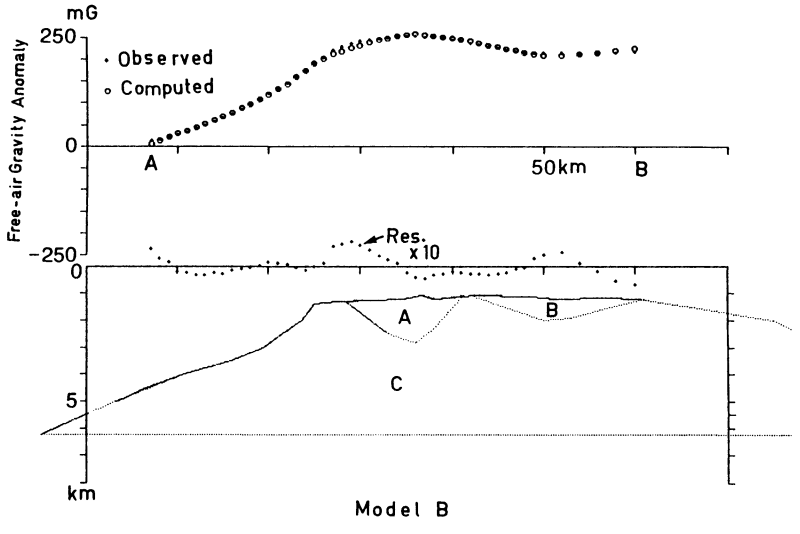

(b)

Fig. 7. Results of two-dimensional gravity/magnetic analyses of profile A–B of Smt-1100. Solid cross marks mean observed anomalies and open circles are calculated ones. Residuals are also shown by solid cross marks. (a) Result of two-dimensional gravity analysis on the assumption of uniform density (Model A); calculated mean density is 2.78 g/cc. Goodness-of-fit ratio is 14.9. (b) Result of two-dimensional gravity analysis on the assumption of non-uniform density (Model B): Calculated density of A is 3.23 g/cc, that of B is 1.56 g/cc and that of C is 2.82 g/cc. Goodness-of-fit ratio is 46.1. (c) Result of two-dimensional magnetic analysis. Effective inclination is assumed to be $-12°$. Magnetization intensity of A is -2.42 A/m and B is -1.30 A/m, C is 5.39 A/m, and D (basement of seamount) is 1.83 A/m. Goodness-of-fit ratio of this model analysis is 2.10.

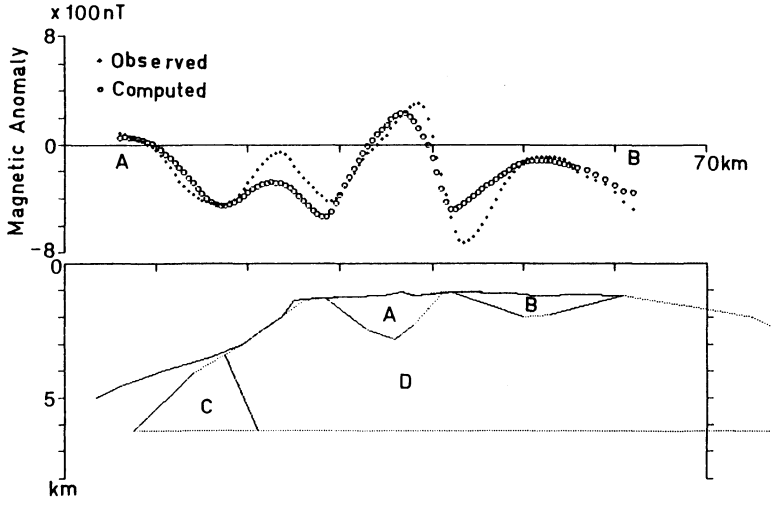

(c)

Fig. 7. (continued).

5. Discussions and Conclusions

5.1 Paleomagnetism

Paleopoles of Smt-948, listed in Table 1, are plotted in Fig. 8. The latitude of the paleomagnetic pole of Smt-948 is nearly constant for each model calculation; on the other hand, the paleopole longitudes range from 305° to 334°. This feature implies an uncertainty of the paleopole position obtained from magnetic analysis for different models. In this case, the goodness-of-fit ratio is conventionally used as the acceptance criteria (HARRISON *et al.*, 1975). The paleomagnetic pole for the model of the maximum goodness-of-fit ratio 2.83 became 57.3°N, 329.5°E (model 3 in Table 1). That of the two-layers model (model 4 in Table 1), whose goodness-of-fit ratio was the same value as model 3, was also very close to this paleomagnetic pole position. As the goodness-of-fit ratio of model 3 satisfies Harrison's acceptance criteria, it is reasonable to assume that the paleomagnetic pole of model 3 represents the reliable VGP of Smt-948. Pacific paleomagnetic poles between the Jurassic and the Cretaceous in age have been presented in various sources (LARSON and CHASE, 1972; HARRISON *et al.*, 1975; CANDE, 1976; GORDON, 1983; COX and GORDON, 1984; SAGER and KEATING, 1984; SAGER and PRINGLE, 1988; YAMAZAKI, 1988). HILDEBRAND and PARKER (1987) reexamined the paleomagnetism of Cretaceous Pacific seamounts using a new method of three-dimensional magnetic inversion. This approach is a superior method for analyzing seamounts of non-uniform magnetization. The calculated mean pole for seamounts dated 65–94 Ma (S1) and for seamounts on 150 Ma or older crust (S2) are plotted by star marks along with

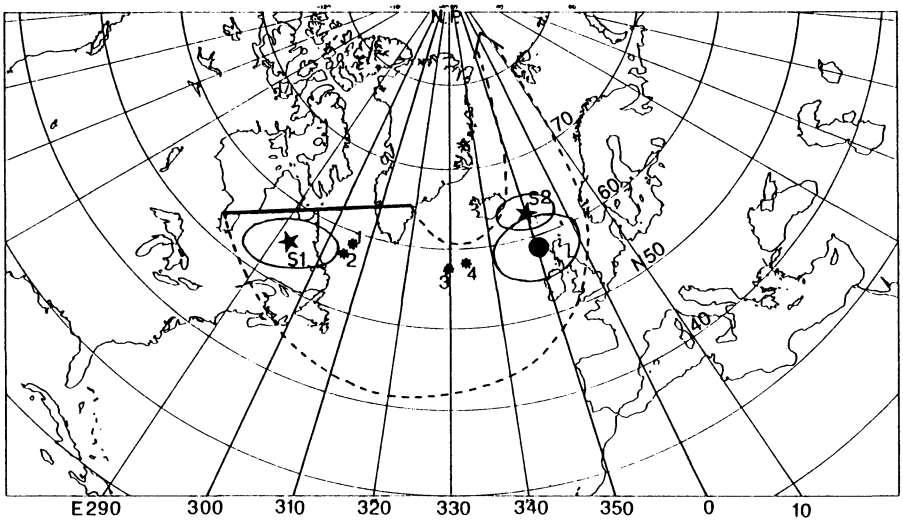

Fig. 8. Paleomagnetic pole positions of Smt-948 and other Cretaceous Pacific seamounts. Pacific plate polar wander path from the Late Jurassic is shown by dotted zone. Thick line shows the paleo-colatitude of DSDP site 307 of 150 Ma old (COX and GORDON, 1984). S1 is mean pole position of seamounts on 150 Ma or older crust and S2 is that of seamounts with mid-late Cretaceous ages (65–94 Ma) (after HILDEBRAND and PARKER, 1987). Large solid circle is mean pole of Cretaceous Pacific seamounts (after HARRISON *et al.*, 1975). Pole positions of Smt-948 are shown by figures corresponding to each model number in Table 1.

the estimated paleomagnetic polar wander path from the Upper Jurassic to the Upper Cretaceous (Fig. 8). The polar wander path compiled by HILDEBRAND and PARKER (1987) indicates that the paleo-Pacific pole moved south during the Lower Jurassic or the Upper Jurassic, moved east during the Middle Cretaceous, and moved north during the Upper Cretaceous.

The paleo-Pacific pole of Smt-948 is located between the mean poles for the 65–94 Ma group and for older groups. This situation suggests that Smt-948 was formed between the Upper Jurassic and the Middle Cretaceous, although it is located in the Jurassic magnetic quiet zone. The above mentioned aspect implies that Smt-948 was formed by igneous activity long after the formation of the seafloor at the ridge crest in the Late Jurassic epoch.

As for Smt-1100, it is difficult to calculate the paleomagnetic pole because of the complicated magnetic anomaly pattern of the seamount and the limited extent of the survey. However, it may be concluded that this seamount was formed during a period of both normal and reversed magnetic epochs. The large size of Smt-1100 suggests that it was formed over a long period of time including several polarity reversals. CANDE *et al.* (1978) reported the existence of magnetic anomalies of low amplitude in the Jurassic magnetic quiet zone, which can be traced back to M29 at 157 my B.P. Smt-1100 is located on a seafloor older than M29, and its magnetiza-

tion is consistent with a low intensity magnetic polarity epoch estimated from the Jurassic magnetic quiet zone. However, to further investigate this assumption, accurate age information is needed for Smt-1100.

5.2 *Structure and origin of flat-topped seamounts*

The origin of the flat-topped seamount is a long-standing problem of paleo-Pacific tectonics. HESS (1946) called them 'guyots' and proposed that they were created in shallow water and emerged at the ridge crest. The seamounts underwent erosion in shallow water and then submerged during drift away from the ridge crest. On the other hand, MENARD (1964, 1984) proposed the well-known hypothesis of the "Darwin Rise" by assuming relief of a guyot above basement given water depth when it was an island. Both assumed that the depth of the flat top was the mean sea water level recorded by shallow water erosion. However, there still remains some ambiguity about the origin of the flat-topped surface. NATLAND (1976) described a possible volcanologic interpretation for the origin of flat-topped seamounts from the results of DSDP site survey cruises of several guyots. It was proposed that many flat-topped seamounts were caused by caldera collapse and filling of the resulting depression by volcanic debris.

The seamount structure inferred from the magnetic and gravity analysis lends support to this hypothesis. The modelled structures of Smt-948 and Smt-1100 suggest the structure of a caldera formation filled by lava. It is noteworthy that no coral reef material was dredged or photographed on the surface of Smt-1100. Additionally, the small knolls on the flat top suggest the occurrence of submarine volcanic activity. These characteristic features imply support for the constructional volcanism hypothesis which assumes that the flat top can be generated by submarine volcanic activity instead of by shallow water erosion. However, the constructional volcanism hypothesis itself does not exclude the possibility that the flat top was formed at sea level, as is shown from a morphological study of the Galapagos volcanoes (NORDLIE, 1973). In fact, sub-rounded basaltic pebbles, an indicator of shallow water erosion, were dredged from the slope break of Smt-1100. This paper does not intend to exclude the shallow water erosion hypothesis for the flat top, but instead to attract attention to an alternative explanation derived from magnetic and gravity modeling. The origin of the flat top is controversial and an important subject related to the vertical crustal movement of the paleo-Pacific Ocean. To solve this problem, the internal structure of guyots must be illuminated by other sources of data.

The author would like to express his hearty thanks to Captain Hideo Okabe and the staff of the S/V Takuyo for their enthusiasm and assistance in surveying, which gave him the opportunity for the present study. He is also very grateful to Mr. Misao Tamaki and Mr. Akira Asada of the Marine Survey Division of the JHD for their useful information about dredged samples and sea-bottom photographs.

The author is much indebted to Dr. W. W. Sager and Dr. Kensaku Tamaki for their critical reading and valuable comments on the manuscript.

REFERENCES

CANDE, S. C., A paleomagnetic pole from late Cretaceous marine magnetic anomalies in the Pacific, *Geophys. J. R. astr. Soc.*, **44**, 547–566, 1976.

CANDE, S. C., R. L. LARSON, and J. L. LABRECQUE, Magnetic lineations in the Pacific Jurassic quiet zone, *Earth Planet. Sci. Lett.*, **41**, 434–440, 1978.

COX, A. and R. G. GORDON, Paleolatitudes from paleomagnetic data from vertical cores, *Rev. Geophys.*, **22**, 47–72, 1984.

FRANCHETEAU, J., C. G. A. HARRISON, J. G. SCLATER, and V. VACQUIER, Magnetization of Pacific seamount: A preliminary polar curve for the Northeastern Pacific, *J. Geophys. Res.*, **75**, 2035–2061, 1970.

GEOGRAPHICAL SURVEY INSTITUTE, Establishment of the Japan gravity standardization net 1975, *J. Geod. Soc. of Japan*, **22**, 65–76, 1976.

GORDON, R. G., Late Cretaceous apparent polar wander of the Pacific Plate: evidence for a rapid shift of the Pacific hotspots with respect to the spin axis, *Geophys. Res. Lett.*, **10**, 709–712, 1983.

HARRISON, C. G. A., A seamount with a nonmagnetic top, *Geophysics*, **36**, 349–357, 1971.

HARRISON, C. G. A., R. D. JARRARD, V. VACQUIER, and R. L. LARSON, Palaeomagnetism of Cretaceous Pacific seamounts, *Geophys. J. R. astr. Soc.*, **42**, 859–882, 1975.

HESS, H. H., Drowned ancient islands of the Pacific Basin, *Am. J. Sci.*, **244**, 772–791, 1946.

HILDEBRAND, J. A. and R. L. PARKER, Paleomagnetism of Cretaceous Pacific seamounts revisited, *J. Geophys. Res.*, **92**, 12695–12712, 1987.

LARSON, R. L., and C. E. CHASE, Late Mesozoic evolution of the western Pacific Ocean, *Geol. Soc. Am. Bull.*, **83**, 3627–3644, 1972.

LEPICHON, X. and M. TALWANI, Gravity survey of a seamount near 35°N 46°W in the north Atlantic, *Marine Geology*, **2**, 262–277, 1964.

MCNUTT, M., Nonuniform magnetization of seamounts: a least squares approach, *J. Geophys. Res.*, **91**, 3686–3700, 1986.

MENARD, H. W., *Marine Geology of the Pacific*, 271 pp., McGraw Hill, New York, 1964.

MENARD, H. W., Origin of Guyots: The Beagle to Seabeam, *J. Geophys. Res.*, **89**, 11117–11123, 1984.

NATLAND, J. H., Possible volcanogenic explanations for the origin of flat-topped seamounts and ridges in the Line Islands and Mid-Pacific Mountains, *Initial Rep. D.S.D.P.*, **33**, 779–787, 1976.

NAYUDU, Y. R., A new hypothesis for origin of guyots and seamount terraces, in *The Crust of the Pacific Basin*, edited by G. A. Macdonald and H. Kuno, pp. 171–180, AGU, Washington, D. C., 1962.

NORDILE, B. E., Morphology and structure of the western Galapagos volcanoes and a model for their origin, *Geol. Soc. Am. Bull.*, **9**, 2931–2955, 1973.

OZIMA, M., M. HONDA, and K. SAITO, ^{40}Ar-^{39}Ar ages of guyots in the Western Pacific and discussion of their evolution, *Geophys. J. R. astr. Soc.*, **51**, 475–485, 1977.

RICHARDS, M. L., V. VACQUIER, and G. D. VANVOORHIS, Calculation of the magnetization of uplifts from combining topographic and magnetic surveys, *Geophysics*, **32**, 678–707, 1967.

SAGER, W. W. and B. H. KEATING, Paleomagnetism of Line Island seamounts: evidence for late Cretaceous and early Tertiary volcanism, *J. Geophys. Res.*, **89**, 11135–11151, 1984.

SAGER, W. W. and M. S. PRINGLE, Mid-Cretaceous to early Tertiary apparent polar wander path of the Pacific plate, *J. Geophys. Res.* (Allan Cox Memorial Volume), 1988 (in press).

SAGER, W. W., G. T. DAVIS, B. H. KEATING, and J. A. PHILPOTTS, A geophysical and geologic study of Nagata Seamount, northern Line Islands, *J. Geomag. Geoelectr.*, **34**, 283–305, 1982.

SCHIMKE, G. R. and C. G. BUFE, Geophysical description of a Pacific ocean seamount, *J. Geophys. Res.*, **73**, 559–569, 1968.

SMOOT, N. C., Guyots of the Dutton Ridge at the Bonin/Mariana Trench Juncture as shown by multi-beam surveys, *Jour. Geol.*, **91**, 211–220, 1983.

TALWANI, M., Computation with the help of a digital computer of magnetic anomalies caused by bodies of arbitrary shape, *Geophysics*, **30**, 797–817, 1965.

UEDA, Y., Geomagnetic study on seamounts Daiiti-Kasima and Katori with special reference to a

subduction process of Daiiti-Kasima, *J. Geomag. Geoelectr.*, **37**, 601–625, 1985.

UYEDA, S. and M. RICHARDS, Magnetization of four Pacific seamounts near the Japanese Islands, *Bull. Earthq. Res. Inst.*, **44**, 179–213, 1966.

WILSON, W. D., Speed of sound in sea water as a function of temperature, pressure and salinity, *J. Acoust. Soc. Am.*, **32**, 641–644, 1960.

YAMAZAKI, T., Magnetization of Erimo Seamount, *J. Geomag. Geoelectr.*, **40**, 715–728, 1988.